Poly(vinylidene fluoride-hexafluoropropylene) polymer electrolyte for paper-based and flexible battery applications

Nojan Aliahmad,[1,2] Sudhir Shrestha,[1,2] Kody Varahramyan,[1,2] and Mangilal Agarwal[1,2,3,a]

[1]*Department of Electrical & Computer Engineering, Indiana University-Purdue University Indianapolis (IUPUI), Indianapolis, IN, 46202, USA*

[2]*Integrated Nanosystems Development Institute (INDI), Indiana University-Purdue University Indianapolis (IUPUI), Indianapolis, IN, 46202, USA*

[3]*Department of Mechanical Engineering, Indiana University-Purdue University Indianapolis (IUPUI), Indianapolis, IN, 46202, USA*

(Received 25 February 2016; accepted 30 May 2016; published online 7 June 2016)

Paper-based batteries represent a new frontier in battery technology. However, low-flexibility and poor ionic conductivity of solid electrolytes have been major impediments in achieving practical mechanically flexible batteries. This work discuss new highly ionic conductive polymer gel electrolytes for paper-based battery applications. In this paper, we present a poly(vinylidene fluoride-hexafluoropropylene) (PVDH-HFP) porous membrane electrolyte enhanced with lithium bis(trifluoromethane sulphone)imide (LiTFSI) and lithium aluminum titanium phosphate (LATP), with an ionic conductivity of 2.1×10^{-3} S cm^{-1}. Combining ceramic (LATP) with the gel structure of PVDF-HFP and LiTFSI ionic liquid harnesses benefits of ceramic and gel electrolytes in providing flexible electrolytes with a high ionic conductivity. In a flexibility test experiment, bending the polymer electrolyte at 90° for 20 times resulted in 14% decrease in ionic conductivity. Efforts to further improving the flexibility of the presented electrolyte are ongoing. Using this electrolyte, full-cell batteries with lithium titanium oxide (LTO) and lithium cobalt oxide (LCO) electrodes and (i) standard metallic current collectors and (ii) paper-based current collectors were fabricated and tested. The achieved specific capacities were (i) 123 mAh g^{-1} for standard metallic current collectors and (ii) 99.5 mAh g^{-1} for paper-based current collectors. Thus, the presented electrolyte has potential to become a viable candidate in paper-based and flexible battery applications. Fabrication methods, experimental procedures, and test results for the polymer gel electrolyte and batteries are presented and discussed. [http://dx.doi.org/10.1063/1.4953811]

Broad applications of bendable electronics have led to an increased attention toward the development of flexible solid-state lithium ion batteries.[1–4] Flexible batteries in the forms of micro-batteries, printable batteries, and stretchable batteries have been reported.[5,6] Recent advancements in paper electronics have shown much potential in delivering commercial paper-based devices for a wide range of applications.[7] However, these efforts have been impeded by the lack of flexible, non-liquid-based batteries that are compatible with paper-based platforms. Despite recent improvements, fabrication of a complete solid, paper-based lithium ion battery remains a challenge.[8,9]

The typical use of liquid electrolyte in lithium ion batteries has been one of the major challenges in the integration of batteries into paper-based devices. On the other hand, ceramic electrolytes lack

[a]Corresponding author. Email: agarwal@iupui.edu; 755 W Michigan St. UL 1140, Indianapolis, IN 460202, USA; Ph: +1-317-278-9792; Fax: +1-317-274-1024.

of the flexibility is also a limiting factor in their use for such devices.[10,11] The motivation of this work is to create a new highly ionic conductive polymer gel electrolyte with LATP (ceramic) and LiTFSI (ionic liquid) for paper-based product applications. The porous structure in the presented electrolyte was created by using glycerol, which represents a new and a simpler method of improving porosity in battery electrolytes.[12] Polymer gel electrolytes have shown promise as they are mechanically flexible, light-weight, and long-lasting. Polymers such as PVDF-HFP and polyethylene oxide (PEO) have been considered the best-suited for solid electrolytes due to their high ionic conductivity and stable material properties within a lithium ion assembly. Previously, ionic conductivity of a PVDF-HFP mixture with an alkali salt and PVDF-HFP electrolyte soaked in ionic liquids have been shown to be in the rage of 10^{-3} S cm^{-1}.[13–15] PVDF-HFP has a polar semi-crystalline structure with amorphous domains that trap electrolyte and provide an ability to transport ions.[16] Infusing an alkali salt inside the cross-linking polymer structure has the potential to provide the ionic conductivity for the polymer membrane. In the presented work, LATP and LiTFSI ionic solution in ethylene carbonate (EC) and diethyl carbonate (DEC) were chosen for their high ionic conductivity, high working voltage window (up to 4 V), and high chemical stability.[17–19] It has also been shown that creation of porous structures in electrolyte membranes increases ionic liquid uptake, thereby increasing the ionic conductivity.[19] Thus in the presented work, porous PVDF-HFP membrane was introduced with the use of glycerol.

Another challenge in achieving flexible batteries for paper-based devices has been the difficulty in developing paper-compatible current collectors. CNT has been studied to overcome such challenges: improvements have been made with reported capacities up to 153.5 mAh g^{-1} and columbic efficiency up to 90.6%.[8,20–22] Despite these recent improvements, these devices still use liquid-based electrolytes and expensive CNT current collector fabrication processes. In the presented work, we use a conductive paper current collector fabricated from paper fibers coated with CNT (CNT-microfiber paper).[9,23,24] The CNT-microfiber paper preserves the porous structure, making it suitable for flexible applications.

This paper therefore demonstrates the implementation of a paper-based battery that utilizes a PVDF-HFP polymer gel electrolyte and CNT-microfiber paper current collectors. To test the ionic conductivity of the polymer gel electrolyte, it was used to fabricate batteries with both (i) standard metallic current collectors followed by (ii) CNT-microfiber paper current collectors.

PVDF-HFP, glycerol, and N-Methyl-2-pyrrolidone (NMP) were mixed with 2-5% LATP (by weight of PVDF-HFP) and stirred in normal atmospheric conditions for 12 hours. PVDF-HFP/LATP polymer gel electrolyte membranes were casted and subsequently dried in air, followed by drying in a vacuum oven at 50°C. The resulting polymer membranes were soaked in liquid electrolyte solution consisting of one mole LiTFSI dissolved in a 1:1 volume ratio solution of EC:DEC. The membranes were then dried in an argon filled glove box. All procedures were carried out at room temperature unless noted otherwise.

The CNT-microfiber current collectors used in this work were fabricated from wood microfibers, each coated with CNT through a layer-by-layer (LbL) nanoassembly process, described in detail elsewhere.[9,23,24] The LbL nanoassembly technique allows the construction of a composite multilayered coating at nanoscale through the alternate deposition of oppositely charged polyelectrolytes and/or nanoparticles. Aqueous dispersions of poly(3,4-ethylenedioxythiophene)-poly(styrenesulfonate) (PEDOT-PSS) conductive polymer (3 mg ml^{-1}) and carbon nanotubes (25 μg ml^{-1}) were used as the anionic polyelectrolyte components, while poly-(ethyleneimine) (PEI) (3 mg ml^{-1}) was used as cationic component.[24] Coating microfibers with two bi-layers of PEI/CNT alternating with two bi-layer of PEI/PEDOT-PSS achieved the desired conductivity. Following CNT-coating, the wood microfibers were assembled into paper sheets (CNT-microfiber paper), and subsequently used as current collectors, described in detail elsewhere.[9] CNT-microfiber paper preserves the important characteristics of the paper, such as texture and porous structure, while reducing CNT utilization to only 0.2% by weight.[9]

LTO and LCO were purchased from Sigma Aldrich. Carbon Black KS6 and super P lithium were purchased from Timcal. LTO (or LCO), Carbon Black KS6, and PVDF-HFP were stirred and dissolved in NMP forming a thick solution. The electrode solutions were then sprayed over the current collectors and dried in a vacuum oven. The mass loading for both of the active materials (LTO and LCO) were 8-9 mg/cm^2. Two types of current collectors were used: (i) metallic (aluminum

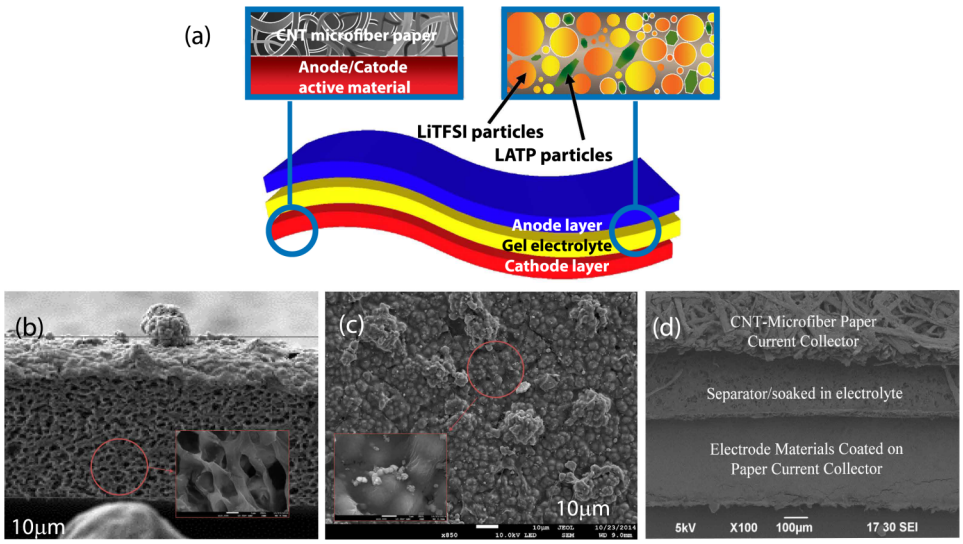

FIG. 1. (a). Schematic shows the presented paper-based polymer gel electrolyte battery assembly. SEM images of the polymer gel electrolyte: (b) the cross-section of the membrane (inset shows the porous structure of the membrane), and (c) the surface of the membrane. The thickness of membrane is ~70 μm. (d) FESEM image showing the three layers of the paper-based PVDF-HFP electrolyte battery.

and copper) and (ii) CNT-microfiber paper. The CNT-microfiber paper provides conductive porous structures for flexible lithium ion batteries and it has been shown previously that electrode materials on the CNT microfiber current collector fabricated in this manner exhibit better flexibility over metallic current collectors.[9] Fig. 1(a) shows a battery assembly with a CNT-microfiber current collector. Here, the middle layer, between top (anode) and bottom (cathode) electrode layers represents the polymer gel electrolyte. The left inset represents CNT-microfiber paper with a coating of electrode material and the right inset depicts porous PVDF-HFP polymer membrane containing ionic liquids and lithium salts. All battery fabrication steps as well as electrolytes encapsulation for impedance measurements were conducted in an argon filled glovebox.

The characterization results for morphology, structure, electrolyte uptake, and ionic conductivity of the polymer gel electrolyte, and the battery results with metallic and CNT-microfiber paper current collectors are presented and discussed in this section. Formation of size-controlled pores was achieved using glycerol as a plasticizer in the polymer-membrane and by residual drying at a constant temperature, and analyzed by FESEM. Addition of glycerol increases the viscosity of the solution and prevents crystallization by separating polymer from the solvents while the membrane is still wet, resulting in the porous structure.[25,26] Fig. 1 shows FESEM images of the (b) cross-section and (c) surface of the fabricated polymer gel electrolyte. The cross-sectional image reveals the porous nature of the PVDF-HFP membrane with uniform pore distribution with an average size ~ 1 μm. The surface of the polymer gel electrolyte (Fig. 1(c)) demonstrates the uniformity of the membrane surface and an even distribution of the lithium salts. Even though some peaks are observed, no surface fractures or other evidence of damage are present. However, the surface peaks may contribute to an increase in internal cell resistance and may contribute to capacity fade.

Dispersion of salts within the polymer gel electrolyte membrane was observed using energy dispersive X-ray spectroscopy (EDS). Fig. 2(a), taken over the cross-section of the electrolyte membrane, shows traces of sulfur in LiTFSI (yellow) (sulfur is unique to LiTFSI) and phosphorus in LATP (green) (PVDF-HFP does have phosphorus in it. However, the brightness of green dots and their random distribution in the sample indicate that they are traces of LATP). Fig. 2(b) shows a trace for LiTFSI (sulfur, yellow) which is uniformly distributed, while Fig. 2(c) shows a trace for LATP (phosphorous, green). The larger LATP particles prevent over-crystallization of the polymer, thereby further aiding the ionic conductivity of the polymer gel electrolyte. LATP acts as a polar filler in the polymer structure reducing crystallinity of the PVDF-HFP film. The normalized

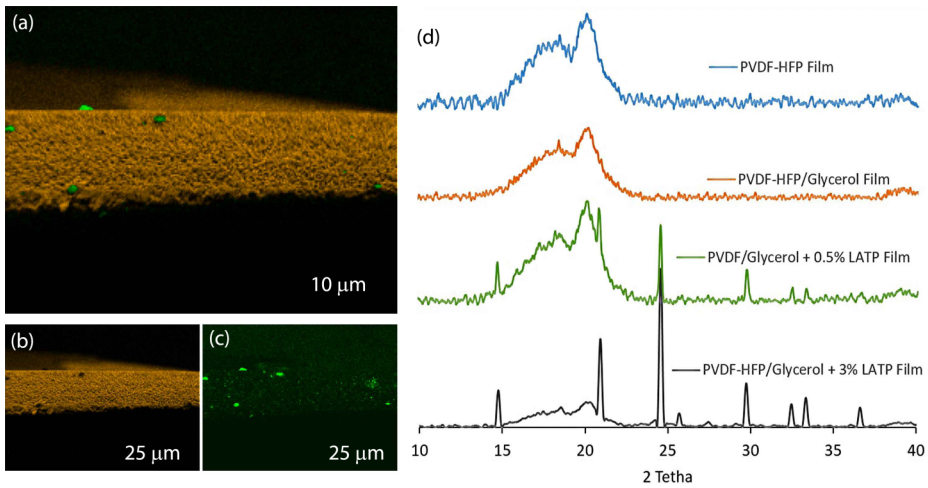

FIG. 2. EDS of the electrolyte membrane cross-section: (a) Trace of all materials, (b) Yellow pixels represent trace of sulfur in LiTFSI, and (c) Bright green pixels represent within the cross-section represent trace of phosphorus in LATP, and (d) XRD results for different concentration of LATP in PVDF-HFP films.

XRD results of the PVDF-HFP films with no LATP, 0.5% by wt LATP and 3% by wt LATP are shown in Fig. 2(d). The peaks observed at 2θ = 18.4° and 20° demonstrate the crystal phase of the PVDF-HFP, and peaks at 14.7° and 21° are attributed to the LATP.[27,28] After adding the glycerol to the PVDF-HFP the peak at 20° became wider. Furthermore, by increasing the amount of LATP the peaks at 14.7° and 21° became sharper while the peaks at 18.4° and 20° became wider. Here the crystallinity of the PVDF-HFP is reduced after adding glycerol and LATP. Here the transfer of protons in the membrane takes place because of the aggregation of Li+ ions from both LiTFSI and LATP in the polymer membrane.[27] Increasing the amount of polar ceramics such as LATP makes a polar medium inside the polymer structure and reduces the crystalline (non-polar) phase of the fabricated films.[28,29]

PVDF-HFP membranes with 1, 2, and 3% by weight concentration of LATP were fabricated and electrolyte uptakes of these membranes tested as follows. Membranes were cut to a predefined size and soaked in a LiTFSI/EC/DEC solution (1 mol, 1:1 by weight). No significant change in electrolyte uptake was observed; the polymer maintained absorption of (450 ± 30)% by weight. When the concentration of the LATP increases by up to 3%, the ionic conductivity of the polymer gel electrolyte improves by 20%. However, higher concentration of the LATP leads to reduction in membrane ionic conductivity.[4]

FTIR results for (a) PVDF-HFP, (b) PVDF-HFP/LATP, and (c) PVDF-HFP/LATP/LITFSI are presented in Fig. 3. The peaks observed at 2750-3000 cm^{-1} and 840-880 cm^{-1}, which occur in all three plots (indicated as "1" in Fig. 3), demonstrate that PVDF-HFP remains in polar form.[28] The peak at 1200-1300 cm^{-1} in plot (a) indicates C-F bonding in PVDF-HFP, which provides segmental movements inside the polymer and enhances the ionic conductivity.[15,18] Sharp peaks at 500-700 cm^{-1} (indicated as "2" in plots (b) and (c)), are for LATP. In addition, a peak of LATP is observed at 980 cm^{-1}, which is due to the P-O bonds in the structure (indicated as "2" in plots (b) and (c)).[14] Peaks for LiTFSI, observed at 1140 cm^{-1} and 1490 cm^{-1} (indicated as "3" in plot (c)), demonstrate that the LiTFSI is dissolved into the gel structure.[30,31] The peaks at 1600-1700 cm^{-1} (indicated as "4" in plot (c)) show the trapping of ionic liquid within the polymer gel structure.[32] Bands 879 and 841 cm^{-1} visible on plots (b) and (c) identify the β and γ phases of the PVDF-HFP, respectively, indicating the amorphous structure of the polymer. The symmetric and asymmetric out of plane deformations of SO_2 group in LiTFSI structure are also visible at 1138 and 617 cm^{-1} bands respectively. In addition, C═O vibration is observed at 1734 cm^{-1}. The C-H stretching, visible at 1420-1440 cm^{-1}, identifies the aggregation of lithium compound in the polymer membrane.[28,33]

Next, electrical impedance spectroscopy (EIS, Solarton Galvanostat) tests of the electrolyte were conducted using stainless steel electrodes in an argon filled glove box. The amplitudes of the

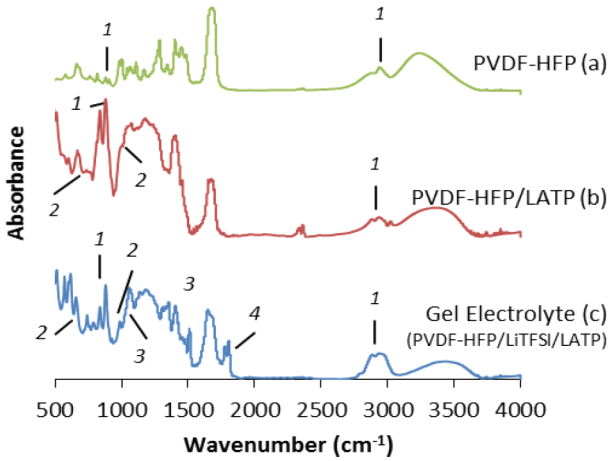

FIG. 3. FTIR results of (a) PVDF-HFP, (b) PVDF-HFT/LATP, and (c) PVDF-HFP/LATP/LiTFSI (polymer gel electrolyte).

DC potential for these measurements were 0.5 mV and frequency range from 100 mHz to 1 MHz. The ionic conductivity of the polymer gel electrolyte was measured to be up to 2.1×10^{-3} S cm^{-1} for 100 μm thick and 2.8×10^{-3} S cm^{-1} for 280 μm thick, respectively. Fig. 4(a) shows the ionic conductivities of these polymer gel electrolytes. In addition, a bending test was conducted and ionic conductivity re-measured. The conductivity of the electrolyte decreased by 14% after it was placed inside a pouch cell and bent at 90° and straightened for 20 times. The decrease in conductivity due to bending is attributed to surface deformation of the polymer, and loss due to migration of the trapped ionic liquid away from the bent areas. Further examination of the electrolyte after the bending test also revealed shallow surface fractures on the polymer around the bent region. The lithium transference number of the electrolyte, measured using stainless steel and lithium electrodes as described by Zhao et al.,[33] was observed to be 0.967.

Next, tests for ionic conductivities of the paper-based and metallic LTO/LCO cell with the polymer gel electrolyte were conducted. The Warburg model was used to determine the ohmic resistance (R_s) and charge-transfer resistance (R_{ct}) of metallic and CNT-microfiber paper-based LTO/LCO batteries. Fig. 5(b) shows the ionic conductivities of two full-cell lithium ion devices fabricated with the gel electrolyte, and using metallic and CNT-microfiber paper current collectors. Inset of Fig. 5(b) shows the equivalent circuit of the cell using Warburg model. These cells used 100 μm thick polymer gel electrolytes. The calculated R_s and R_{ct} are 0.15 Ω and 5.78 Ω for metallic current collector-based batteries and 7.92 Ω and 40 Ω for paper-based batteries, respectively. The higher R_s for paper-based cell is attributed to a higher dielectric constant of paper current collectors and imperfect contact between the electrodes and electrolyte membrane. In addition, the surface roughness of the paper-based electrodes reduces the effective contacts between the polymer gel electrolyte and the electrodes.

LTO/LCO full cells were fabricated using copper and aluminum metallic current collectors and tested for the voltage range of 0.8 to 2.5 V with C 5^{-1} rate. The capacities of the metallic current collector cell for the 1st and 10th cycles are shown in Fig. 5(a). The 1st cycle charge capacity was measured to be 123 mAh g^{-1} and discharge capacity was measured as 85 mAh g^{-1}. These capacities are comparable to the LTO/LCO battery capacities published in literature.[8,9] A high drop in capacity of 18% from the 1st to 2nd cycle was observed. However, after the 2nd cycle the drops in capacity in consecutive cycles were less than 4% each. The drop in capacity from 1st to 3rd and 1st to 5th cycles were 21.4% and 28.1%, respectively, while the drop in capacity from 2nd to 10th cycle was 24%. The drop in capacity is attributed to the extraction of free ions in the polymer membrane causing a reduction in the ionic conductivity. In addition, the formation of a solid electrolyte interface (SEI) layer, unbalanced capacity between anode and cathode (resulting from the use of spray method), and formation of lithium over electrolyte during the charge/discharge cycle that causes trapping of the lithium ions over the surface of the polymer gel electrolyte, may also contribute to the capacity drop.[34,35]

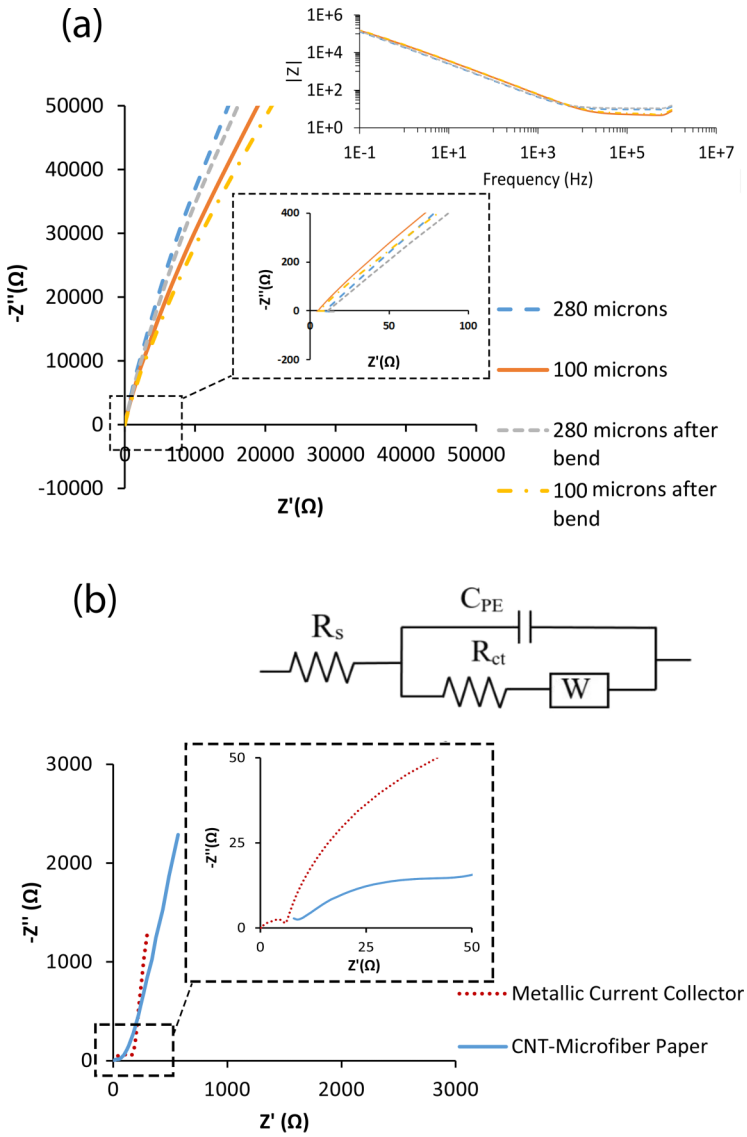

FIG. 4. (a) Impedance measurements of the polymer gel electrolyte (before and after the bending), (b) The inset shows the equivalent circuit of the cell, and frequency vs impedance plot of the polymer gel electrolytes.

Full cells using CNT-microfiber current collectors were fabricated and tested. An FESEM image showing the layers of CNT-microfiber current collectors and electrolyte membrane is shown in Fig. 1(d). It was observed that the active materials formed a uniform layer over the paper substrates. This uniform layer is more resistive to bends and fractures due to the porous nature of the CNT-microfiber paper.[9] The charge and discharge capacity curves for the paper-based cell are shown in Fig. 5(b). Maximum charge and discharge capacities of 99.5 mAh g^{-1} and 75.6 mAh g^{-1}, respectively, were achieved. This charge capacity is 24% lower than the charge capacity of metallic current collector cells presented above. The higher internal resistance of the cell which was discussed above is attributed to a lower capacity and slightly lower voltage observed in the CNT-microfiber current collector cells as compared to metallic current collector cells. Other factors causing this drop may be attributed to a higher dielectric constant of paper current collectors, imperfect contact between the electrodes and electrolyte membrane and lower effective contacts between the polymer gel electrolyte and the electrodes.

Furthermore, the imperfect contact between the active material layer and polymer gel electrolyte reduces the ionic conductive paths, which also contributes to a reduction in the overall

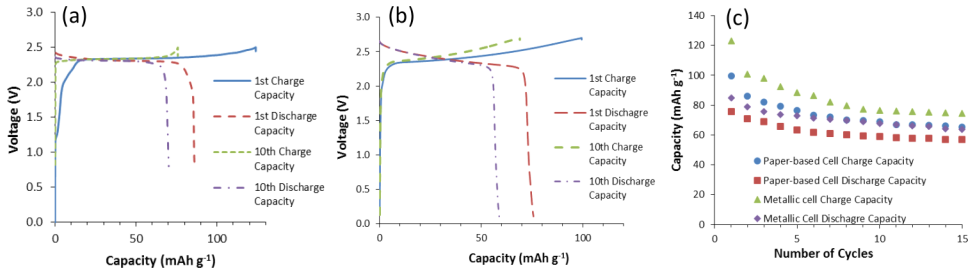

FIG. 5. (a). 1st and 10th charge/discharge cycles of metallic current collector LTO/LCO electrodes and PVDF-HFP electrolyte cell. (b) Charge/discharge characteristics of paper-based PVDF-HFP electrolyte battery (c) The cycle life of the polymer gel electrolyte cells made with metallic and paper-based and metallic current collectors.

capacity.[34,35] However, the capacities for the paper current collector batteries reported here, which use polymer gel electrolyte (thus, have all solid construction), are comparable with the capacities for preciously reported paper batteries that use liquid electrolytes and LTO/LCO electrode materials.[9] Similar to the metallic current collector batteries discussed in the previous section, a high drop in capacity of 13% from 1st to 2nd cycle was also observed in the CNT-microfiber current collector batteries. However, the drop was only 19% from 2nd to 10th cycles (compared with 18% and 24% respectively for first to second and second to 10th cycles for the metallic current collector data). As described above for metallic current collector cells, SEI formation, material stabilization, and variations in electrode mass loadings due to the spray method are attributed for these capacity drops. In addition, having the CNT in the electrodes can also increase the chance of the SEI formation in presence of the EC and DEC solvents, over the electrodes.[36] Fig 5(c) show the capacity of the paper-based and metallic cells for the first 15 cycles. The capacity of the cells decreased sharply after the 15th cycle due to the SEI and lithium dendrite formation.[33,34] The cyclic performance needs to be improved for wider applications of the developed batteries. Efforts to improve the cycle life of the cells are currently being pursued. It should be noted that the electrode materials over CNT-microfiber current collectors provide better flexibility compared to metallic current collectors as described in detail elsewhere.[9] Most importantly, the use of paper-based CNT-microfiber current collectors and a polymer gel electrolyte makes the presented battery assembly better suited for integration in paper-based platforms.

A PVDF-HFP polymer gel electrolyte with a high ionic conductivity and its application in paper-based batteries consisting of CNT-microfiber paper current collectors have been presented. The electrolyte consists of a highly porous PVDF-HFP membrane enhanced with LATP and LiTFSI ionic solution, and ionic conductivity of 2.1×10^{-3} S cm^{-1} was achieved. Combining of the high ionic conductivity property of ceramic and mechanical flexibility of polymer gel structure has been demonstrated to provide flexible gel electrolyte with high ionic conductivity, an enabling feature for paper-based battery development. The electrolyte membrane was fabricated into regular and paper-based cells using LTO and LCO electrode materials, and performances were studied. Capacities up to 123 mAh g^{-1} for metallic and 99.5 mAh g^{-1} for CNT-microfiber current collector based devices, respectively, were achieved. The difference in the charge/discharge plateau between the paper-based and metallic cells is due to the difference in the total impedance of the cells.[32] The higher internal resistance of the paper-based battery is attributed to a lower capacity from first to second cycle. Efforts to overcoming these challenges and further improving the cycle-life of the developed batteries are ongoing. While the capacity and performances for the paper-based battery need improvement, the solid paper-based battery shows promises in many applications that require only limited power, such as RFID, wireless sensors, electrochromic displays, and paper-based functional electronics.

Acknowledgments are due to the Integrated Nanosystems Development Institute (INDI) for providing the facilities for this research, including the JEOL7800F Field Emission Scanning Electron Microscope awarded through NSF grant MRI-1229514 and Bruker D8 Discover X-Ray Diffraction Instrument, which was awarded through NSF grant MRI-1429241. The authors would like to thank

Dr. Yadong Liu for his assistance in the laboratory and Dr. Daniel Minner for his assistance with the FESEM instrument.

[1] A.L. Chun, Nature Nanotechnology **305**, 1038 (2007).
[2] Z. Song, T. Ma, R. Tang, Q. Cheng, X. Wang, D. Krishnaraju, R. Panat, C.K. Chan, H. Yu, and H. Jiang, Nature communications **5**, 3140 (2014).
[3] J. Fuller, A. Breda, and R. Carlin, Journal of the Electrochemical Society **144**, 67 (1997).
[4] J.W. Fergus, Journal of Power Sources **195**, 4554 (2010).
[5] J.M. Tarascon and M. Armand, Nature **414**, 359 (2001).
[6] C. Wang, W. Zheng, Z. Yue, C.O. Too, and G.G. Wallace, Advanced Materials **23**, 3580 (2011).
[7] D. Tobjörk and R. Österbacka, Advanced Materials **23**, 1935 (2011).
[8] L. Hu, J.W. Choi, Y. Yang, S. Jeong, F. La Mantia, L.F. Cui, and Y. Cui, Proceedings of the National Academy of Sciences **106**, 21490 (2009).
[9] N. Aliahmad, M. Agarwal, S. Shrestha, and K. Varahramyan, IEEE Transactions on Nanotechnology **12.3**, 408 (2013).
[10] F.M. Gray, *Solid polymer electrolytes* (VCH New Tork etc, 1991).
[11] J.B. Goodenough and Y. Kim, "Challenges for rechargeable Li batteries," Chemistry of Materials **22.3**, 587 (2009).
[12] L. Shi, R. Wang, Y. Cao, D. Liang, and J. Tay, Journal of power sources **315**, 195 (2008).
[13] H. Ye, J. Huang, J.J. Xu, A. Khalfan, and S.G. Greenbaum, Journal of the Electrochemical Society **154**, A1048 (2007).
[14] J. J. Song, Y. Wang, and C. Wan, Journal of Power Sources **77**, 183 (1999).
[15] D. Saikia and A. Kumar, Electrochimica acta **49**, 2581 (2004).
[16] J. H. Cao, B. K. Zhu, and Y. Y. Xu, Journal of membrane science **281**, 446 (2006).
[17] M. Moshkovich, M. Cojocaru, H. Gottlieb, and D. Aurbach, Journal of Electroanalytical Chemistry **497**, 84 (2001).
[18] Y. Liang, Z. Lin, Y. Qiu, and X. Zhang, Electrochimica Acta **56**, 6474 (2011).
[19] M. Yang and J. Hou, Membranes **2**, 367 (2012).
[20] A. Mansourizadeh and A. Ismail, International Journal of Greenhouse Gas Control **5**, 640 (2011).
[21] J. Wang, L. Li, C.L. Wong, and S. Madhavi, Nanotechnology **23**, 495401 (2012).
[22] C. Liu and H. M. Cheng, Journal of Physics D: Applied Physics **38**, R231 (2005).
[23] M. Agarwal, Q. Xing, B.S. Shim, N. Kotov, K. Varahramyan, and Y. Lvov, Nanotechnology **20**, 215602 (2009).
[24] M. Agarwal, Y. Lvov, and K. Varahramyan, Nanotechnology **17**, 5319 (2006).
[25] S. Rajabzadeh, T. Maruyama, T. Sotani, and H. Matsuyama, Separation and Purification Technology **63**, 415 (2008).
[26] S. Atchariyawut, C. Feng, R. Wang, R. Jiraratananon, and D. Liang, Journal of Membrane Science **285**, 272 (2006).
[27] P. G. Bruce, *Solid State Electrochemistry* (Cambridge University Press, 1997), Vol. 5.
[28] S. Abbrent, J. Plestil, D. Hlavata, J. Lindgren, J. Tegenfeldt, and Å. Wendsjö, Polymer **42**, 1407 (2001).
[29] Fergus and W. Jeffery, Journal of Power Sources **195**, 4554 (2010).
[30] A. Daneshkhah, S. Shrestha, M. Agarwal, and K. Varahramyan, Sensors and Actuators B: Chemical **221**, 635 (2015).
[31] S. H. Yeon, K. S. Kim, S. Choi, J.-H. Cha, and H. Lee, Journal of Physical Chemistry B **109**, 17928 (2005).
[32] S. Jeschke, M. Mutke, Z. Jiang, B. Alt, and H. D. Wiemhöfer, ChemPhysChem **15**, 1761 (2014).
[33] J. Zhao, L. Wang, X. He, C. Wan, and C. Jiang, Journal of Electrochemical Society **155**, A292 (2008).
[34] P. Arora, R. E. White, and M. Doyle, Journal of Electrochemical Society **145**, 3647 (1998).
[35] A. Du Pasquier, I. Plitz, J. Gural, F. Badway, and G. G. Amatucci, Journal of Power Sources **136**, 160 (2004).
[36] B. J. Landi, M. J. Ganter, C. D. Cress, R. A. DiLeo, and R. P. Raffaelle, Energy & Environmental Science **6**, 638 (2009).